How to remove diverges from the QED-Hartree approximation

1990 J. Phys. A: Math. Gen. 23 3969

(http://iopscience.iop.org/0305-4470/23/17/026)

J. Phys. A: Math. Gen. 23 (1990) 3969–3982. Printed in the UK

How to remove divergences from the QED–Hartree approximation

A Hamm† and D Schütte

Institut für Theoretische Kernphysik der Universität Bonn, D-5300 Bonn 1, Federal Republic of Germany

Received 19 September 1989, in final form 22 March 1990

Abstract. The removal of divergences from the formal Hartree approximation of the vacuum charge density in quantum electrodynamics is discussed as a generalization of a procedure known from perturbative calculations in the Furry picture. A new diagrammatical justification of this procedure is given. Numerical tests are reported which show that the usual approach in the Furry picture can be modified to meet the requirements of approximations inspired by many-body theory. The calculations are based on the sum-over-modes expression of vacuum charge density—not in the usual version as spectral asymmetry, but in a formulation which takes into account corrections for the influence of the free Dirac sea. Owing to numerical expense, a self-consistent computation without further approximations in the sums over modes proves to be impracticable.

1. Introduction

The computation of the level displacement due to radiative corrections in light hydrogen-like atoms is one of the well known standed tests of Feynman–Dyson perturbative QED [1]. But in the case of heavy atoms with large nuclear charge numbers, Z, one has to renounce a perturbative treatment of the potential which influences the atomic electrons. The usual procedure in this case [2] is defined in the framework of Furry-picture QED, which is a hybrid of a non-perturbative theory as far as the external potential is concerned, and a perturbation theory for the self-interaction of the electron field.

Hartree–Fock-like procedures were proposed to dispose of even the remaining perturbative feature [3] (see also [4] for a related discussion in the context of nuclear matter) and to make possible the treatment of many-electron atoms [5].

A QED approximation scheme only makes sense, if a consistent and practicable accompanying renormalization procedure is given. This usually means:

(i) Some regularization scheme is used to prevent divergency problems during

† Present address: Fachbereich Physik, Universität Essen, D-4300 Essen 1, Federal Republic of Germany.

0305-4470/90/173969+14$03.50

the evaluation of the formal approximation.

(ii) A prescription of modifying the regularized expression is given in such a way that the removal of the regularization becomes possible. The modifications must be suitable for being absorbed in a change from bare to physical parameters (the actual renormalization). Uniqueness is obtained by consideration of physical requirements (e.g. symmetries).

The renormalization procedure in Feynman–Dyson perturbative QED is exemplary. On the other hand, it is not quite clear how to deal with the Hartree–Fock-like approximations.

In the present article we propose an extension of a strategy used in the context of Furry-picture QED [6, 7]. The idea of that strategy is to add an intermediate step after the regularization, but before the actual renormalization. In this step attention is directed to the dependence of the regularized (but not renormalized) non-perturbative approximation on the external potential:

The first few orders of the formal expansion into powers of the external potential contain all the divergences which result from a removal of the cut-off. For each given cut-off, this precarious low-order part can be determined by comparative calculations with weak fields.

After subtraction of that part, the remaining, substantially non-perturbative part converges as the cut-off is removed. The subtracted low-order part, however, need not be exploited in the framework of the non-perturbative approximation but can be replaced by a perturbative calculation of corresponding order. We shall call the strategy sketched above 'separation of the low-order dependence'. In practice, 'low-order' often means 'first-order'. We shall then speak of 'separation of the linear dependence' then.

The method has a technically very important merit: the regularization scheme used for separating the low-order dependence need not be the same as the one used for the actual renormalization. In particular, the condition of compatibility with the gauge invariance is no longer in force. Thus, one can work with a simple cut-off regularization.

In the following section a consistent definition of a Hartree approximation to the QED vacuum charge density is formulated including renormalization along the lines of separation of the linear dependence.

Section 3 contains a new graphical justification of the separation strategy. It may also be useful for an analysis of applicability of the strategy to more advanced approximation schemes.

In section 4 numerical evidence is given that separation of the linear dependence in principle works, not only in the procedures of [6, 7], but also in calculations with sums over discrete modes. The interest in this result originates in the fact, that defining non-perturbative approximation schemes in terms of sums over discrete modes is advantageous from a heuristical point of view: procedures inspired by non-perturbative methods in a non-relativistic many-body theory naturally arise in this form.

An evaluation of the Hartree approximation might shed light upon the controversially discussed question about what happens in very strong ('critical') external fields, where the bound states descend to the Dirac sea (see [2] and references therein for the most prominent answer to that question). However, in the arguments of the following sections we assume external potentials of moderate strength to avoid those critical situations as well as the problem of non-self-adjointness, which appears in (non-realistic) Coulomb potentials with nuclear charge numbers $Z > 118$.

2. Definition of the QED–Hartree approximation of the vacuum charge density

It is well known that in non-relativistic many-body theory the Hartree approximation can be obtained from the Dyson equation for the exact electron Green function by taking into account, instead of all proper self-energy insertions, only an exact electron-propagator tadpole [8]. This procedure can be transferred (almost) literally to formal QED in the external potential V_Z of an atomic nucleus with charge number Z. The resulting Hartree equation for the electron propagator is shown graphically in figure 1(*a*).

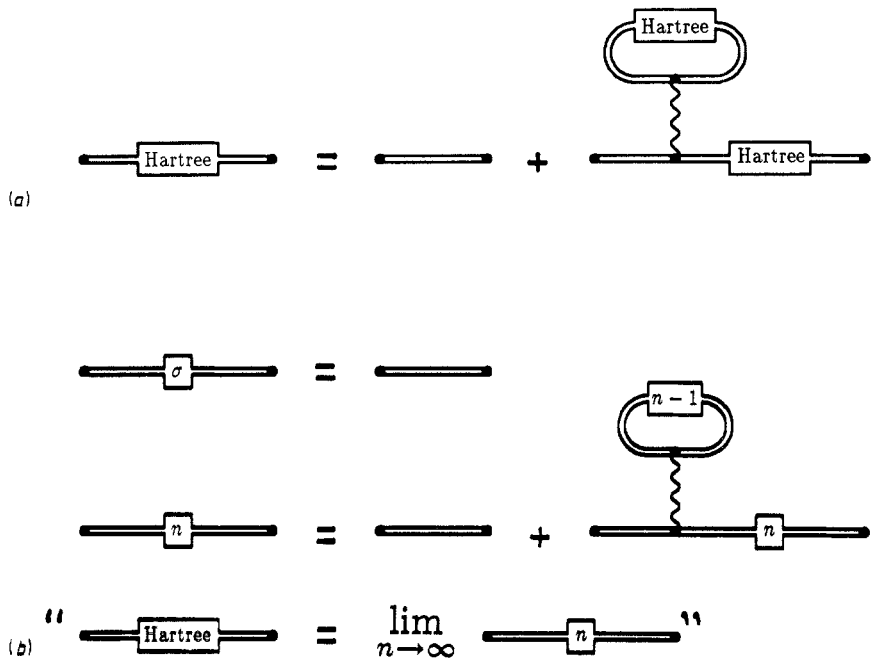

Figure 1. Graphical representation of (*a*) the (unrenormalized) Hartree equation and (*b*) its formal iterative solution.

We recall the definitions of the propagators entering such graphs, in which the usual Feynman rules apply. We use Feynman gauge fixing, Gaussian units, and standard notations [1, 2].

Wavy lines represent the free photon propagators D_0, the solution with Feynman boundary conditions of

$$\partial_\lambda \partial^\lambda D_0^{\mu\nu}(x,y) = 4\pi\delta(x-y)g^{\mu\nu}.$$

Double lines stand for electron propagators, S_Z, in an external potential, V_Z, which are the solutions with Feynman boundary conditions of

$$(i\gamma^\mu \partial_\mu - e\gamma^0 V_Z - m)S_Z(x,y) = \delta(x-y).$$

The free electron propagator is the special case S_0 with $V_0 \equiv 0$ and is represented by a single line. If $Z \neq 0$ we refer to S_Z as Furry electron propagators. Further

approximations to the exact electron propagator are depicted by double lines with labelled boxes.

The Hartree equation has to be solved iteratively (figure 1(*b*)).

To be more tangible, we now turn to the eigenvalue problem which results from a mean-field *ansatz* for the electron propagator in a discretized spectral representation (which requires suitable boundary conditions, see section 4). This *ansatz*, inserted into the iteration prescription of figure 1(*b*), yields (for details see [5, 9]):

$$(-\boldsymbol{\alpha}\cdot \mathrm{i}\boldsymbol{\partial} + \beta + \mathcal{V}_Z^{(n)}(\boldsymbol{x}))\,\varphi_{Z,i}^{(n)}(\boldsymbol{x}) = \varepsilon_{Z,i}^{(n)}\,\varphi_{Z,i}^{(n)}(\boldsymbol{x}) \tag{1}$$

where

$$\mathcal{V}_Z^{(0)}(\boldsymbol{x}) = eV_Z(|\boldsymbol{x}|) \tag{2}$$

and

$$\mathcal{V}_Z^{(n+1)}(\boldsymbol{x}) = eV_Z(|\boldsymbol{x}|) + \int \mathrm{d}^3y\,\frac{e^2\rho_Z^{(n)}(\boldsymbol{y})}{|\boldsymbol{x}-\boldsymbol{y}|} \tag{3}$$

with

$$\rho_Z^{(n)}(\boldsymbol{y}) = \Big[\sum_j\Big]\varphi_{Z,j}^{(n)*}(\boldsymbol{y})\,\varphi_{Z,j}^{(n)}(\boldsymbol{y}). \tag{4}$$

In the last equation, $[\sum](\ldots)$ is an abbreviation of $\frac{1}{2}(\sum_{\mathrm{occ}}(\ldots) - \sum_{\mathrm{unocc}}(\ldots))$, where the two sums extend over the occupied and unoccupied one-particle states of the configuration considered. For instance, for an N-electron atom in its ground state, the occupied states are the Dirac sea (DS) states ($\varepsilon_{Z,i}^{(n)} < -m$) and the N lowest bound states ($|\varepsilon_{Z,i}^{(n)}| < m$). Especially for $N = 0$, equation (4) (which then measures the spectral asymmetry) gives a formal expression of the approximate vacuum electron density in the presence of an external field, when taking into account the electron self-interaction by a Hartree iteration.

All these formal results have been known for a long time. A very ample treatment, moreover allowing for Fock's exchange term, can be found in [5].

Instead of (4) we are going to use a slightly different formal expression of the charge density [9]:

Formally, one has the symmetry of the free Dirac spectrum:

$$\sum_{\mathrm{DS}}\varphi_{0,j}^*(\boldsymbol{y})\,\varphi_{0,j}(\boldsymbol{y}) = \sum_{\text{non-DS}}\varphi_{0,j}^*(\boldsymbol{y})\,\varphi_{0,j}(\boldsymbol{y})$$

and the base independence of traces:

$$\sum_{\mathrm{all}}\varphi_{Z,j}^{(n)*}(\boldsymbol{y})\,\varphi_{Z,j}^{(n)}(\boldsymbol{y}) = \sum_{\mathrm{all}}\varphi_{0,j}^*(\boldsymbol{y})\,\varphi_{0,j}(\boldsymbol{y}).$$

Thus we obtain

$$\begin{aligned}\Big[\sum\Big]\varphi_{Z,j}^{(n)*}(\boldsymbol{y})\,\varphi_{Z,j}^{(n)}(\boldsymbol{y}) &= \sum_{\mathrm{occ}}\varphi_{Z,j}^{(n)*}(\boldsymbol{y})\,\varphi_{Z,j}^{(n)}(\boldsymbol{y}) - \frac{1}{2}\sum_{\mathrm{all}}\varphi_{Z,j}^{(n)*}(\boldsymbol{y})\,\varphi_{Z,j}^{(n)}(\boldsymbol{y}) \\ &= \sum_{\mathrm{occ}}\varphi_{Z,j}^{(n)*}(\boldsymbol{y})\,\varphi_{Z,j}^{(n)}(\boldsymbol{y}) - \frac{1}{2}\sum_{\mathrm{all}}\varphi_{0,j}^*(\boldsymbol{y})\,\varphi_{0,j}(\boldsymbol{y}) \\ &= \sum_{\mathrm{occ}}\varphi_{Z,j}^{(n)*}(\boldsymbol{y})\,\varphi_{Z,j}^{(n)}(\boldsymbol{y}) - \sum_{\mathrm{DS}}\varphi_{0,j}^*(\boldsymbol{y})\,\varphi_{0,j}(\boldsymbol{y}).\end{aligned}$$

We arrive at the following expression:

$$\rho_Z^{(n)}(y) = \sum_{\text{occ}} \varphi_{Z,j}^{(n)*}(y)\,\varphi_{Z,j}^{(n)}(y) - \sum_{\text{DS}} \varphi_{0,j}^{*}(y)\,\varphi_{0,j}(y). \tag{5}$$

This form explicitly shows a correction term due to the influence of the free Dirac sea in addition to the naive adoption of the expression from non-relativistic many-body theory. (Note, that the same correction term can also be obtained following somewhat different arguments from [4].) Besides, it is advantageous for computational use, since only the *occupied* bound states are involved.

However, the problem with formal expressions like (4) or (5) is, that they involve infinite sums. Thus, we are forced to start up the machinery of renormalization outlined in the introduction.

We regularize the sums over modes in equation (5) by the introduction of a lower energy cut-off $-\Lambda_C$. Removing the cut-off amounts to the limit $\Lambda_C \to \infty$.

Since the formal procedure (1)–(4) or (5) is iterative, one has two choices concerning the succession of iteration and removal of divergences: One could either repeat the iteration till self-consistency for each given cut-off and study the cut-off dependence of these self-consistent results, or one could alternatively remove the divergences already in each iteration step, hoping for convergence of this modified iteration. Yet, even if both these alternatives work, it is not obvious at all, whether they lead to identical results.

It should be clear, however, that only the second choice will offer a practicable way of removing the divergences; otherwise one would have to run through many self-consistency procedures (parametrically varying the cut-off) instead of one, certainly exceeding the feasibility of numerical treatment.

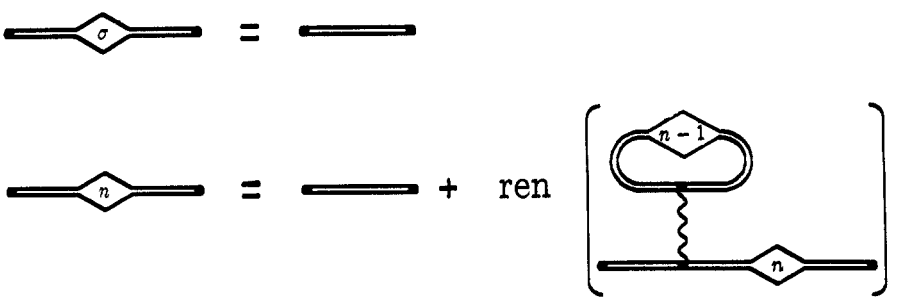

Figure 2. Graphical representation of the renormalized Hartree iteration procedure.

Thus we now concentrate on the removal of divergences in each step of the iteration. We are going to replace the iteration prescription of figure 1(*b*) by that of figure 2. This means that instead of the ill-defined density $\rho_Z^{(n)}(y)$ from equation (5) we have to look for a renormalized nth-step vacuum charge density $\rho_Z^{(n)z\,\text{ren}}(y)$ which makes sense when inserted in equation (3).

Here we shall take advantage of a fact which was first used by Rinker and Wilets [6] and Gyulassy [7] in the context of an evaluation of the vacuum charge density in the first order Furry approximation, and which we shall corroborate in the next section.

For the moment we are content with stating the following fact.

After regularization with a sufficiently large cut-off Λ_C, the charge density (5) shows a linear dependence on the effective potential $\mathcal{V}_Z^{(n)}(\boldsymbol{y})$ as long as Z is very small:

$$\rho_Z^{(n)}(\boldsymbol{y};\Lambda_C) = C(\boldsymbol{y})\,\mathcal{V}_Z^{(n)}(\boldsymbol{y}) \qquad \text{for } Z \text{ near } 1$$

where, for each fixed $\boldsymbol{y}$, $C(\boldsymbol{y})$ is a constant independent of Z.

We extrapolate to larger values of Z and define

$$\rho_Z^{(n)1}(\boldsymbol{y};\Lambda_C) := \frac{\mathcal{V}_Z^{(n)}(\boldsymbol{y})}{\mathcal{V}_1^{(n)}(\boldsymbol{y})}\,\rho_1^{(n)}(\boldsymbol{y};\Lambda_C) \qquad \text{for all } Z. \tag{6}$$

We can hereby split up the regularized charge density into a linear part, and a part of higher order in the effective potential:

$$\rho_Z^{(n)}(\boldsymbol{y};\Lambda_C) = \rho_Z^{(n)1}(\boldsymbol{y};\Lambda_C) + \rho_Z^{(n)>}(\boldsymbol{y};\Lambda_C). \tag{7}$$

The interest in this split-up stems from the fact that the limit

$$\rho_Z^{(n)>}(\boldsymbol{y}) := \lim_{\Lambda_C\to\infty} \rho_Z^{(n)>}(\boldsymbol{y};\Lambda_C) \tag{8}$$

exists under the condition that $\mathcal{V}_Z^{(n)}(\boldsymbol{y})$ is non-singular at $\boldsymbol{y} = 0$ (which precludes an ideal Coulomb potential). This is the key fact of the strategy of separation of the linear dependence.

On the other hand, $\rho_Z^{(n)1}(\boldsymbol{y};\Lambda_C)$ diverges as $\Lambda_C \to \infty$. But the renormalized contribution of first order in an external potential ($\mathcal{V}_Z^{(n)}(\boldsymbol{y})$ in our case) to the vacuum charge density is well known from one-loop perturbative QED [1]; we denote this Uehling contribution by $\rho_Z^{(n)\,\mathrm{Ueh}}(\boldsymbol{y})$.

Thus, the required renormalized nth-step vacuum charge density is obtained as

$$\rho_Z^{(n)\,\mathrm{ren}}(\boldsymbol{y}) = \rho_Z^{(n)\,\mathrm{Ueh}}(\boldsymbol{y}) + \tilde{\rho}_Z^{(n)>}(\boldsymbol{y}). \tag{9}$$

The part $\tilde{\rho}_Z^{(n)>}(\boldsymbol{y})$ may differ from $\rho_Z^{(n)>}(\boldsymbol{y})$ from equation (8) by an unphysical but finite contribution proportional to $(\mathcal{V}_Z^{(n)})^3$, which may be generated depending on the details of regularization. If it is present, it will show up in a discrepancy for small Z of (9) with the results of third-order perturbation theory. In this case the linear extrapolation (6) has to be replaced by a cubic one. Then, only the part of higher-than-third order has to be determined non-perturbatively and added to the results of third-order perturbative calculations.

Equation (9) completes the definition of a divergence-free Hartree iteration procedure for the QED vacuum in the presence of a non-singular external potential.

3. Diagrammatic analysis of the divergences in an unrenormalized step of the Hartree iteration

In this section we give a diagrammatic power-counting justification of the facts stated in the last part of the previous section, especially the existence of the limit (8).

The idea is to study the dependence of divergences on the effective potential by correlating the divergences with divergent graphs with known dependence on the potential. Although this justification is not a strict mathematical proof, it is more systematic than the arguments usually found in this context; this gives rise to the hope that it might help to transcribe the strategy for other approximation schemes.

We particularly stress that the arguments—even though diagrammatical—are not perturbative.

We now investigate which ultraviolet divergences may occur in the diagram within brackets in figure 2, containing an insertion of a renormalized propagator loop (from the previous step) via a photon line.

The method of this investigation is to study those diagrams which result from the replacement of the $(n-1)$th-step propagator by one of the diagrams of the lower row of figure 3, introducing dotted lines for the renormalized effective potential $V_Z^{(n-1)}$.

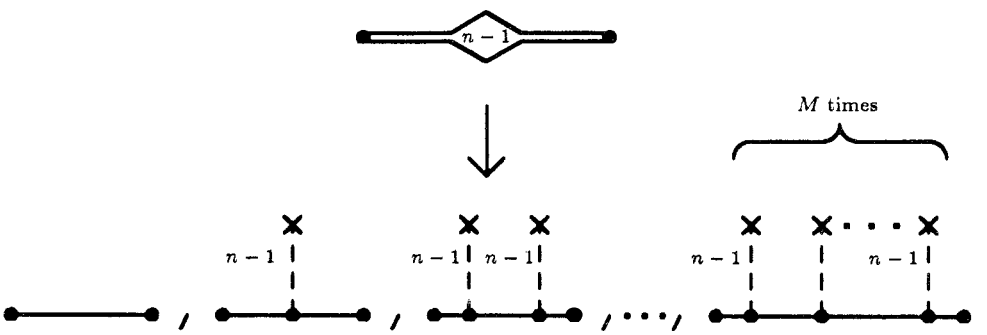

Figure 3. Analytical substitution of the $(n-1)$th-step propagator.

This most definitely does not mean that we are going to expand this propagator into powers of the effective potential (which would be a perturbative argument); we do not aim at an evaluation of the diagrams. Rather, in the substantiation of our strategy, we follow the arguments from chapter 11 of [10]:

In coordinate representation the ultraviolet divergences of the propagator loop originate in the short-distance singularities of the $(n-1)$th-step electron propagator $S_Z^{(n-1)}(x,y)$. We concentrate on the singular part, $S_{Z,\mathrm{s}}$, of this propagator. Depending on the diagram (i.e., the corresponding integral) which is analysed, the singular part can be decomposed as

$$S_{Z,\mathrm{s}} = S_{Z,\mathrm{ss}} + S_{Z,\mathrm{sh}}. \tag{10}$$

Here, $S_{Z,\mathrm{ss}}$, the serious contribution to the singular part, is a sum of M terms of decreasing gravity of singularity:

$$S_{Z,\mathrm{ss}} = \sum_{i=1}^{M} S_{Z,\mathrm{si}} \tag{11}$$

and $S_{Z,\mathrm{sh}}$, the harmless contribution to the singular part, is an even less singular expression. The last part is called harmless because its singularity is so weak that

the integral being under examination would exist, if $S_{Z,s}$ were replaced by $S_{Z,sh}$. An actual realization of the decomposition (10) and (11) requires the choice of some regularization scheme by which the sum (11) can be obtained from a 'perturbative' extraction of M singular terms. The fact that M is finite is essential, because we must not use an infinite perturbative expansion. (For an illustrative example of a similar decomposition of the free scalar propagator $S_0^{scal}(x)$ we refer to [10], where dimensional regularization is used. The $x = 0$ singularity of this propagator can be interpreted as the combined effect of a $x = 0$ pole in non-integer dimensions and a singular behaviour in the transition to the physical dimension. In non-integer dimensions the decomposition (11) is equivalent to a sum over decreasing powers of $1/x$.)

All we need to know about $S_{Z,si}$ is that its short-distance behaviour tallies with that of the ith term of the lower row of figure 3. Now, the structure of possible ultraviolet divergences can be discussed by confining our attention to the part $S_{Z,ss}$, or more precisely, by studying the effect of its short-distance behaviour on the integral. This is exactly what is done by the replacement indicated in figure 3.

After this replacement, we interpret the diagrams in momentum space, and connect the free ends of the potential lines and of the photon line of the insertion to one auxiliary vertex. We so maintain the applicability of the usual graph-theoretical [11] identification of the first Betti number of the graph with the number of independent integrations in view of momentum conservation at each vertex.

Taking into account Furry's theorem (cf [1]) we conclude that the only diagrams, Γ_i ($i = 1,3,5,\ldots$), which could contribute to the divergence of the RHS of figure 2 show the structure depicted in the first row of figure 4.

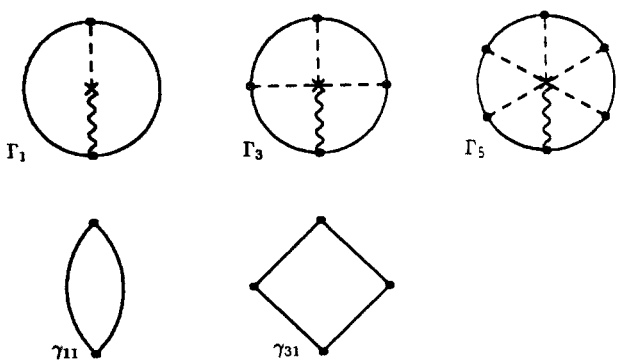

Figure 4. Graphs relevant to the detection of divergences.

Here, power-counting methods can be used to reveal possible divergences: Only those diagrams Γ_i can cause divergences, which have subdiagrams, $\gamma_{ij} \subseteq \Gamma_i$, with non-negative superficial degree of divergence, $\omega(\gamma_{ij}) \geq 0$.

The superficial degree of divergence, $\omega(\gamma)$, describes the behaviour of the integrands corresponding to the diagram γ, when all the momenta of integration grow large simultaneously:

$$\omega(\gamma) = 4\mu(\gamma) + N_e(\gamma)\deg(S_0) + N_{ph}(\gamma)\deg(D_0) + N_A(\gamma)\deg(A_Z^{(n)}). \tag{12}$$

In this equation $\mu(\gamma)$, $N_e(\gamma)$, $N_{ph}(\gamma)$, and $N_A(\gamma)$ are the first Betti number, the number of electron lines, of photon lines, and of potential lines, respectively.

The ultraviolet degree of a function $f : \mathbb{R}^m \to \mathbb{R}^l$ is defined as

$$\deg(f) = \max\left\{\nu \in \mathbb{Z} : \lim_{\lambda\to\infty} \lambda^{-\nu} f(\lambda \underline{p}) \neq 0,\ \underline{p} \in \mathbb{R}^m - \{0\}\right\} \tag{13}$$

and therefore

$$\deg(S_0) = -1 \tag{14}$$

and

$$\deg(D_0) = -2. \tag{15}$$

On the other hand, for a distribution of the form $g(p) = \delta(p_0) f(\underline{p})$, where

$$p = (p_0, \underline{p}) \in \mathbb{R} \times \mathbb{R}^m$$

we define

$$\deg(g) = \deg(f) - 1. \tag{16}$$

This definition takes into account that the Dirac function effectively reduces the dimension of the integral by one.

Since we are dealing with static potentials, the four-dimensional Fourier transform $A_Z^{(n)}$ of $\mathcal{V}_Z^{(n)}$ has the form of g in equation (16), with f being the three-dimensional Fourier transform of $\mathcal{V}_Z^{(n)}$. From (13) and (16) we thus obtain

$$\deg(A_Z^{(n)}) = \max\left\{\sigma \in \mathbb{Z} : \lim_{\mu\to 0} \mu^{\sigma}\, \mathcal{V}_Z^{(n)}(\mu \boldsymbol{x}) \neq 0,\ \boldsymbol{x} \in \mathbb{R}^3 - \{0\}\right\} - 3 - 1. \tag{17}$$

If the potential shows a Coulomb $1/r$ singularity at the origin, this degree is

$$\deg(A_{\text{Coul}}) = -3. \tag{18}$$

But with a more realistic model of the charge distribution of the atomic nucleus (cf [2]) which generates the potential, the potential will be finite at the origin:

$$\deg(A_{\text{real}}) = -4. \tag{19}$$

In this case, inserting (14), (15), and (19) into equation (12) and making use of the Euler–Poincaré formula

$$1 - \mu(\gamma) = M(\gamma) - (N_e(\gamma) + N_{\text{ph}}(\gamma) + N_A(\gamma)) \tag{20}$$

where $M(\gamma)$ denotes the total number of vertices of γ, we obtain

$$\omega(\gamma) = 3N_e(\gamma) + 2N_{\text{ph}}(\gamma) + 4(1 - M(\gamma)). \tag{21}$$

From this equation we see, that for the diagrams Γ_j from figure 4

$$\omega(\Gamma_j) = 1 - j. \tag{22}$$

Therefore only the diagram Γ_1 is superficially overall-divergent. (Note that using (18) instead of (19) would result in $\omega(\Gamma_j) = 1$ for each j. Thus, all the Γ_j would be superficially overall-divergent. This shows that for a singular potential there are ultraviolet divergences in all orders of a formal expansion in powers of the potential.)

Among all the subgraphs of the diagrams $\Gamma_1, \Gamma_3, \ldots$ there are only two with non-negative superficial degree of divergence: γ_{11} with $\omega(\gamma_{11}) = 2$ and γ_{31} with $\omega(\gamma_{31}) = 0$ (see figure 4, second row). They are both well known in the context of perturbative calculations [1]: γ_{11} from the Uehling term of vacuum polarization and γ_{31} from the Karplus–Klein term of photon–photon scattering.

If we follow the procedure of equations (6), (7) (separation of the linear dependence), we get rid of the divergences connected with the graphs Γ_1 and γ_{11}. If required we can, as mentioned above, extend the procedure to a separation of the third-order dependence to avoid the possible problems of γ_{31}.

However, this need not be necessary in view of a property of the Karplus–Klein term, which we recall now. The diagram γ_{31} represents, after assigning momenta and orientations to the electron lines in all possible ways, six different graphs. It is well known (see [12]) that the divergent contributions from these graphs cancel mutually, independent of the regularization scheme. But the finite part which remains depends noticeably on the method of regularization.

A sufficient condition for the correctness of the finite result is to respect the gauge invariance in all steps of the regularized calculation (e.g. Pauli–Villars regularization or dimensional regularization).

A simple necessary *a priori* criterion for a regularization which leads to the correct finite part of γ_{31} is not known. So, since we do not want to give up the convenience of free choice for an easy-to-use regularization, we have to check our results *a posteriori*. If there are difficulties with γ_{31}, they show up as inconsistencies with third-order perturbative calculations, as mentioned in the end of the previous section.

4. Numerical test of the first-order subtraction in the context of mode summation

The realization of the approximation scheme outlined in section 2 is an extensive computational task. Before tackling this problem, one should try to get a numerical confirmation that first-order subtraction really removes divergences from the sums over modes; the arguments from the preceding section are encouraging but of course not strictly conclusive, and the fact that the method works in the examples of [6, 7] says little about its applicability to the case of discrete mode summation according to equation (5).

The computation of $\rho_Z^{(0)>}(\boldsymbol{x})$ from equations (8), (7), and (5) for $r := |\boldsymbol{x}|$ not too small (compared with the scale given by the imposed boundary conditions) presents itself as a test of convergence. The restriction concerning r serves the purpose of a comparatively rapid convergence of the sums. Such a test was performed in [9]. We briefly sketch the procedure and the results.

For a central potential $\mathcal{V}_Z^{(n)}(\boldsymbol{x}) = \mathcal{V}_Z^{(n)}(r)$ it is standard [2] to replace equation (1) by the radial Dirac equation, which follows from a separation *ansatz*

$$\varphi^{(n)}_{Z\kappa,\mu,i}(r,\hat{r}) = \frac{1}{r}\begin{pmatrix} G_{Z\kappa,i}(r)\Omega^{\mu}_{j,l_+}(\hat{r}) \\ F_{Z\kappa,i}(r)\Omega^{\mu}_{j,l_-}(\hat{r}) \end{pmatrix} \tag{23}$$

for the solutions of (1) with relativistic angular momentum quantum number κ and magnetic quantum number μ ($j = |\kappa| - \frac{1}{2}$, $l_\pm = j \pm \operatorname{sgn}(\kappa)/2$, Ω^μ_{jl}: spherical spinor).

We obtain a countable set of square integrable solutions to the radial Dirac equation by imposing the boundary condition

$$G_i(R) + F_i(R) = 0$$

for a suitably large 'bag radius' R. (This condition is adopted from the MIT-bag quark model. We also investigated the condition $F_i(R) = 0$ with no noteworthy change in the results.) The radius R has to be larger than the extension of the atomic shell, say $R \geq 10$ Å.

Equation (5) becomes

$$\rho_Z^{(n)}(\boldsymbol{x}) = \frac{1}{e}\sum_{k=1}^{\infty} \rho_{Zk}^{(n)}(r) \tag{24}$$

$$\rho_{Zk}^{(n)}(r) = \frac{-e}{4\pi r^2}\left(\sum_{\mathrm{DS},|\kappa|=k} ((G_{Z\kappa,i}(r))^2 + (F_{Z\kappa,i}(r))^2) - \sum_{\mathrm{DS},|\kappa|=k} ((G_{0\kappa,i}(r))^2 + (F_{0\kappa,i}(r))^2)\right). \tag{25}$$

Even though the RHS expression of equation (25) may exist for all k without renormalization, the sum over k in (24) certainly diverges.

But after renormalization of (25) the $\rho_{Zk}^{(0)}(r)$ rapidly decrease with increasing k (cf [6, 7]). Now the sum in (24) does exist.

As an example of the renormalization of (25) we concentrate on $\rho_{Z1}^{(0)}$.

The regularized but unrenormalized density $\rho_{Z1}^{(0)}(r; \Lambda_C)$ is calculated from (25) by a low-energy cut-off $-\Lambda_C$ in the sums. The decomposition (7) is realized numerically in a particulary simple way if $V_Z(r)$ is proportional to Z, since (6) becomes

$$\rho_Z^{(0)1}(\boldsymbol{y}; \Lambda_C) = Z\rho_1^{(0)}(\boldsymbol{y}; \Lambda_C).$$

Thus,

$$\rho_{Z1}^{(0)>}(r; \Lambda_C) = \rho_{Z1}^{(0)}(r; \Lambda_C) - Z\,\rho_{11}^{(0)}(r; \Lambda_C). \tag{26}$$

The statement to be tested is that this expression converges for $\Lambda_C \to \infty$ to the Furry-picture correction of the one-loop vacuum polarization.

The rate of convergence is expected to increase with r/R. We content ourselves with values $r/R > 1/100$ to get sufficiently rapid convergence, reasonable for the purpose of a test. As a matter of fact, r then has the order of magnitude of $100\lambda\!\!\!^{-}_e$, where the Compton wavelength of the electron

$$\lambda\!\!\!^{-}_e = \frac{\hbar}{m_e c} \approx 3.86 \times 10^{-3}\ \text{Å}$$

gives the range of the neighbourhood of the nucleus, where vacuum polarisation becomes significant. Thus, our test consists of showing that the expression (26) with $r > R/100$ converges to zero.

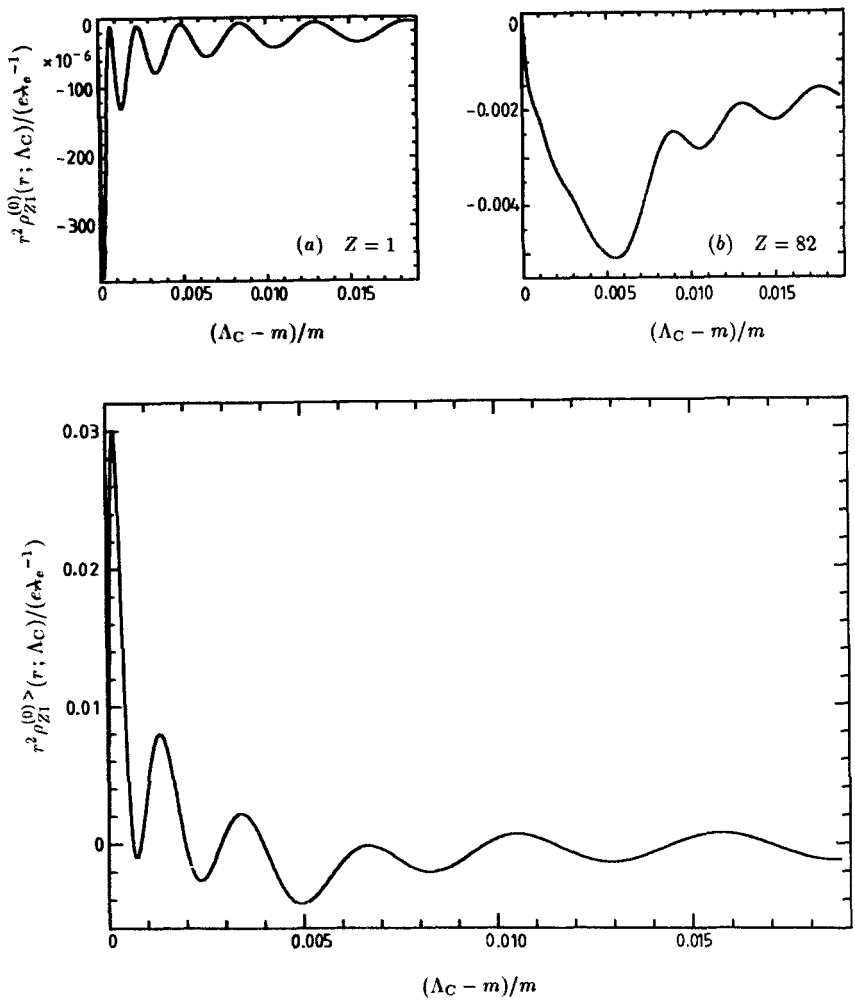

Figure 5. Dependence on the cut-off Λ_C of the $|\kappa| = 1$ parts at a distance $r = 100\lambda\!\!\!^{-}_e$ of (a) the unrenormalized vacuum charge density, $\rho^{(0)}_{Z1}(r;\Lambda_C)$, with $Z = 1$, (b) the unrenormalized vacuum charge density, $\rho^{(0)}_{Z1}(r;\Lambda_C)$, with $Z = 82$, (c) the renormalized correction, $\rho^{(0)>}_{Z1}(r;\Lambda_C)$, to the first-order vacuum charge density with $Z = 82$. The radius of the boundary conditions is $R = 10$Å.

Since in our calculations r is large not only compared to the size of the nucleus but also to $\lambda\!\!\!^{-}_e$, it is sufficient to use an ideal Coulomb potential

$$V_Z^{\mathrm{Coul}}(r) = -Ze/r.$$

Modification of this potential due to the nuclear charge distribution is essential for convergence only for much smaller r.

The Coulomb solutions of the radial Dirac equation can be explicitly written down in terms of confluent hypergeometric functions (see [2,9]). This spares us numerical integration of this differential equation. For a realistic external potential, or higher iterative steps, numerical integration is unavoidable.

Figure 5 shows the result of a computation following equation (26) for $Z = 82$, $R = 10$ Å, $r = 100\lambda\!\!\!^{-}_e$ ($\Rightarrow R/r \approx 25$). Parts ($a$) and ($b$) depict the cut-off dependences

of the two unrenormalized densities in the RHS of equation (26). The largest cut-off used, $\Lambda_C \approx 1.019 m_e$, leads to a restriction of the sums in (25) to about 300 modes each. (To be precise, the curves shown in figure 5 are the smoothed versions of step functions with 300 steps each, according to the discrete values of the cut-off where new modes enter the calculation.) Both curves converge to finite values. Especially for (*b*) we find

$$|r^2 \rho^{(0)}_{Z1}(r)| > 1.2 \times 10^{-3}\, e/\lambda\!\!\!^{-}_e.$$

Figure 5(*c*) shows the resulting density of higher than first order in the external potential: it converges to zero with an accuracy of $10^{-4}\, e/\lambda\!\!\!^{-}_e$.

Precision is limited by the oscillatory behaviour of the curves, which is due to the sharp cut-off. The oscillations can be removed and convergence can be accelerated by implicitly extrapolating the curves (as discussed in [6] in a slightly different context).

The accuracy of our calculation suffices to accomplish the object of the test. For an actual computation the accuracy should be improved by at least three orders of magnitude.

Calculations with larger values of R show that this additional expenditure is barely profitable; the amplitude of the oscillations is decreased relatively little.

The minimal number of modes necessary to detemine the limit $\Lambda_C \to \infty$ is found to be approximately $10\,R/r$ in each sum.

5. Conclusion

Separation of the linear dependence has in principle qualified for removing divergences from sum-over-mode expressions of vacuum charge density. Calculations for distances much smaller than the Compton wavelength of the electron need quite an effort; sums over several millions of modes are required. Concerning the Hartree procedure this means that in each iteration step several millions of solutions to the Dirac equation have to be determined numerically. This hurdle of insurmountable computational effort should be bypassed by introducing some averaging procedure in the sums over modes. In a sense the procedure of [6] can be reinterpreted in this way.

It does not seem likely, for critical external fields, that the results of a Hartree calculation should reveal a qualitative change compared with those within the Furry picture. (Criticism of the widely held ideas of those critical situations could rather be founded on a radical doubt about the applicability of the external field approximation in this case.)

Beyond those more practical questions, the aim of this article has been to plead for raising the separation of the low-order dependence from a special trick in the Furry-picture computation of vacuum polarization to a more general method for renormalizing suitable non-perturbative approximations.

Acknowledgments

Thanks are due to B C Metsch and H R Petry for useful discussions.

References

[1] Itzykson C and Zuber J-B 1980 *Quantum Field Theory* (New York: McGraw-Hill)
[2] Greiner W, Müller B and Rafelski J 1985 *Quantum Electrodynamics of Strong Fields* (Berlin: Springer)
[3] Dietz K and Weymans G 1984 *J. Phys. B: At. Mol. Phys.* **17** 4801
[4] Schütte D 1983 *Nucl. Phys.* A **411** 369
[5] Reinhard P-G, Greiner W and Arenhövel H 1971 *Nucl.Phys.* A **166** 173
[6] Rinker G A and Wilets L 1975 *Phys. Rev.* A **12** 748
[7] Gyulassy M 1975 *Nucl.Phys.* A **244** 497
[8] Fetter A L and Walecka J D 1971 *Quantum Theory of Many-Body Systems* (New York: McGraw-Hill)
[9] Hamm A 1988 *Diplomarbeit* (unpublished) Universität Bonn TK 88 09
[10] Collins J C 1984 *Renormalization* (Cambridge: Cambridge University Press)
[11] Nakanishij N 1970 *Graph Theory and Feynman Integrals* (New York: Gordon and Breach)
[12] Jauch J M and Rohrlich F 1976 *The Theory of Photons and Electrons* (Berlin: Springer)